Advances in Pharmacology and Pharmacy 13(4A): 770-784, 2025 http://www.hrpub.org
DOI: 10.13189/app.2025.130703

Exploring the Potential of a Novel Antiviral Candidate: Molecular Insights into Combatting Sexually Transmitted Diseases

Ibrahim Konneh[1], Cenk Serhan Ozverel[2,3], Emine Erdag[2,4,*], Nazife Sultanoglu[2]

[1]Department of Medical Microbiology and Clinical Microbiology, Faculty of Medicine, Near East University, Mersin-10, Turkey
[2]DESAM Research Institute, Near East University, Mersin-10, Turkey
[3]Department of Basic Medical Sciences, Faculty of Dentistry, Near East University, Mersin-10, Turkey
[4]Department of Pharmaceutical Chemistry, Faculty of Pharmacy, Near East University, Mersin-10, Turkey

Received September 29, 2024; Revised March 26, 2025; Accepted September 21, 2025

Cite This Paper in the Following Citation Styles

(a): *[1] Ibrahim Konneh, Cenk Serhan Ozverel, Emine Erdag, Nazife Sultanoglu , "Exploring the Potential of a Novel Antiviral Candidate: Molecular Insights into Combatting Sexually Transmitted Diseases," Advances in Pharmacology and Pharmacy, Vol. 13, No. 4A, pp. 770 - 784, 2025. DOI: 10.13189/app.2025.130703.*

(b): *Ibrahim Konneh, Cenk Serhan Ozverel, Emine Erdag, Nazife Sultanoglu (2025). Exploring the Potential of a Novel Antiviral Candidate: Molecular Insights into Combatting Sexually Transmitted Diseases. Advances in Pharmacology and Pharmacy, 13(4A), 770 - 784. DOI: 10.13189/app.2025.130703.*

Abstract Sexually transmitted diseases (STDs) caused by viruses such as HIV and HCV remain a global health concern. Antiviral resistance is increasing due to viral mutations, necessitating the search for novel therapeutic candidates. This study evaluated the binding affinities and potential efficacy of eleven antiviral drugs and a drug candidate, AVG-388, using *in silico* methods against HIV and HCV target proteins. Molecular docking simulations were performed using AutoDock Vina, followed by MM/PBSA calculations to determine binding free energies. Molecular dynamics simulations were conducted using GROMACS, and Monte Carlo simulations modeled the variability in binding energies. A 3D energy landscape was mapped using Matplotlib, and a multivariate regression analysis was conducted to correlate binding energies with predicted ligand efficacy. As a result, AVG-388 demonstrated consistently strong binding affinities across HIV and HCV targets. The binding energy for HIV reverse transcriptase was -171.15 ± 2.42 kJ/mol and for HCV RdRp NS5B was -226.21 ± 3.25 kJ/mol. Sofosbuvir showed stronger binding for HCV (-256.26 ± 2.36 kJ/mol) but was less effective against HIV. Statistical analysis revealed that AVG-388 outperformed several FDA-approved antivirals, such as Remdesivir and Molnupiravir, in dual-target inhibition potential. The study highlights AVG-388 as a promising broad-spectrum antiviral candidate, demonstrating superior binding affinities for both HIV and HCV. Further *in vitro* and clinical evaluations are necessary to confirm its potential for treating STDs and overcoming resistance to viral infections.

Keywords Sexually Transmitted Diseases, HIV, HCV, Drug Resistance, Molecular Docking, *In silico* Analysis

1. Introduction

This Sexually transmitted diseases (STDs) are infections that can be transmitted between sexual partners through oral, anal, or vaginal contact. Hepatitis C virus (HCV) and human immunodeficiency virus (HIV) are examples of viruses that cause STDs. Untreated infections caused by STDs are highly prevalent and can lead to serious consequences such as cervical cancer, ectopic pregnancy, infertility, and pelvic pain, placing a substantial load on healthcare systems [1].

As of the end of 2023, there were an estimated 39.9 million people globally living with HIV. This includes both

adults and children, with 1.3 million new infections reported in the same year [2, 3]. Additionally, approximately 630,000 people died from AIDS-related illnesses during 2023. The burden of HIV remains highest in the WHO African Region, where the prevalence is around 3.4% of the adult population. Globally, 0.6% of adults aged 15–49 are living with HIV, with significant variations between regions and populations most affected by the virus [2, 3]. The STDs were reported to require an extended period for effective management and treatment [4]. HCV, on the other hand, remains a major global health concern, causing nearly 1 million new infections each year [5]. In 2022, viral hepatitis, including HCV, was responsible for approximately 1.3 million deaths, with HCV accounting for about 17% of these fatalities. Although there has been progress in diagnosis and treatment, only 36% of people living with chronic hepatitis C have been diagnosed, and 20% have received curative treatment [5].

Viral causative STDs can be classified based on the genetic content of the virus as either RNA or DNA viruses [6]. The RNA viruses are subject to frequent mutations, a process that can precipitate the development of resistance to antiviral drugs utilized in clinical settings. These mutations often occur during RNA synthesis, as replication errors are prone to arise due to the absence of proofreading enzymes, analogous to those found in DNA replication processes [6, 7]. The enzymes crucial for the replication process include HIV reverse transcriptase which converts the viral RNA into DNA [8]. It is integrated into the host cell's genome, allowing the virus to replicate. Therefore, inhibitors of reverse transcriptase are key antiretroviral drugs used to treat HIV infection. Furthermore, RNA-dependent RNA polymerase (RdRp) NS5B is a crucial enzyme for the replication of HCV [9]. As a key component of the viral replication machinery, RdRp catalyzes the synthesis of new RNA strands from an RNA template, making it essential for viral genome replication [9]. Due to its central role in the HCV life cycle, NS5B is a highly conserved and attractive target for antiviral drug development. Targeting NS5B can disrupt viral replication, thereby inhibiting the proliferation of the virus within infected cells.

Various treatments have been demonstrated to effectively alleviate the symptoms and slow the progression of STDs [10]. The United States Food and Drug Administration (FDA) has fully or emergently approved numerous antiviral medications. Among these, molnupiravir (Lagevrio), remdesivir (Veklury), and favipiravir (Avigan) have been authorized or approved for emergency use in the treatment of RNA virus infections, including COVID-19, by inhibiting viral RNA replication, particularly in SARS-CoV-2 [11]. Similarly, nirmatrelvir, as part of the Paxlovid combination, has received emergency use authorization for COVID-19 treatment [12]. Entecavir (Baraclude) and sofosbuvir (Sovaldi) are specifically approved for targeting HCV [13]. Ritonavir (Norvir) is primarily used to enhance the efficacy of other antiretrovirals in HIV therapy, while lopinavir, in combination with ritonavir and marketed as Kaletra, is an FDA-approved antiretroviral for HIV/AIDS treatment [13]. Ribavirin (Rebetol) also has applications in HIV treatment regimens when used in combination with other drugs. For influenza, Oseltamivir (Tamiflu) and zanamivir (Relenza) is FDA-approved for treating influenza A and B [14]. On the other hand, AVG-388, a derivative shown to be effective in a respiratory syncytial virus (RSV) mouse model, lacks substantial data on its activity against sexually transmitted viruses [15].

Consequently, the selection of optimally effective alternative drug candidates becomes critical in the fight against viruses that exhibit resistance to existing antiviral medications. In this study, the effectiveness of twelve different antiviral drugs was evaluated against a spectrum of STD viruses HCV, and HIV. The assessment was conducted utilizing *in silico* methods, which allowed for the computational prediction of drug affinity and target selectivity, thereby providing valuable insights into the potential of these antiviral agents to counteract various STD viruses, including those with established drug resistance.

2. Materials and Methods

2.1. Preparation of Dataset

The selected ligands were downloaded from the PubChem database and involved twelve antiviral drugs, namely Remdesivir (PubChem ID: 121304016), Favipiravir (PubChem ID: 492405), Oseltamivir (PubChem ID: 65028), Ritonavir (PubChem ID: 392622), Lopinavir (PubChem ID: 92727), Ribavirin (PubChem ID: 37542), Zanamivir (PubChem ID: 60855), Nirmatrelvir (PubChem ID: 155903259), Entecavir (PubChem ID: 135398508), Sofosbuvir (PubChem ID: 45375808). For the candidate ligand AVG-388 (Sourimant et al., 2022), the chemical structure was initially drawn using ChemDraw Professional 12.0.2 (PerkinElmer, USA). The two-dimensional (2D) structures of the ligands were then created using LigandScout 4.0 (Inte GmbH, Austria) and subsequently converted to mol2 file formats for further processing. The three-dimensional (3D) structures of the viral proteins were obtained from the Protein Data Bank (PDB). Molecular docking simulations were performed using AutoDock Vina (Scripps Research Institute, USA). The docking complexes were visualized and analyzed using Discovery Studio Visualizer Client (BIOVIA, USA), which allowed for detailed examination of the ligand-binding interactions, particularly the amino acid residues involved within the binding site of the viral proteins.

Before the docking simulations, protein structures were optimized through several preparatory steps. These included the removal of water molecules and heteroatoms to simplify the docking environment. Hydrogens were added and classified as polar or nonpolar, ensuring a more accurate protein surface representation. Finally, Gasteiger charges were assigned to all atoms to accurately simulate electrostatic interactions. Once these optimizations were completed, the proteins were converted into PDBQT format for the docking simulations.

2.2. Molecular Docking

In the molecular docking, target proteins from tested viruses were meticulously selected based on their critical roles in viral replication and pathogenesis. These proteins included the reverse transcriptase from HIV and the RdRp NS5B from HCV. The docking process utilized the Lamarckian Genetic Algorithm (LGA) for the iterative refinement of molecular configurations [16]. This approach was employed to minimize the energy landscapes of the docking interactions, thereby facilitating the identification of ligands with optimal binding affinities. The parameters for docking included a grid box size of 30 x 30 x 30 Å to encompass the entire active site of the target protein. Upon completion of the docking simulations, the resultant complexes were analyzed through conformal clustering using a root-mean-square deviation (RMSD) threshold of 2.0 Å to identify the most stable and representative docking poses. The binding affinities of the resulting ligand-protein complexes were quantitatively evaluated in terms of kilocalories per mole (kcal/mol). The detailed examination of the interaction diagrams of docked complexes highlights key interactions between the ligands and their corresponding protein targets.

2.3. Molecular Dynamics and MM/PBSA Calculations

The Molecular dynamics (MD) simulations were performed using GROMACS (version 2020.4, GROMACS Development Team, Stockholm, Sweden) for 100 nanoseconds at 300 K and 1 bar (http://www.gromacs.org/). The AMBER force field was used for proteins, and the GAFF force field was used for ligands. Simulations included TIP3P water molecules, and the Particle Mesh Ewald (PME) method was used for long-range electrostatics [17]. The resulting MD trajectories were used to compute the binding free energies (ΔG) using the Molecular Mechanics/Poisson-Boltzmann Surface Area (MM/PBSA) methodology. The binding free energies were determined for each complex according to a previously published procedure [18]. The calculated free energies were presented in the equation as follows;

$$\Delta G_{bind} = \Delta G_{complex} - (\Delta G_{target\ protein} + \Delta G_{ligand}) \quad (1)$$

In the equation, ΔG_{bind} was defined as the binding free energy, $\Delta G_{complex}$ as the free energy of the protein-ligand complex, ΔG_{target} protein, and ΔG_{ligand} as the total energies of the protein and ligand respectively, in a solvent environment over a simulation period of 100 nanoseconds (ns).

2.4. Statistical and Multivariate Regression Analysis

Statistical comparisons were made using GraphPad Prism (version 8.0, GraphPad Software, San Diego, CA, USA). P-values were calculated for binding energy differences using ANOVA with post hoc Tukey tests ($P<0.05$ considered significant). A multivariate regression analysis [19] was performed to evaluate the relationship between the binding energies of HIV and HCV proteins and ligand efficacy. The model was fitted using Python's scikit-learn (version 0.24.2). The multivariate regression plot was generated, showcasing the relationship between binding energies and predicted performance.

2.5. *In silico* Off-Target Analysis

The off-target prediction of AVG-388 was conducted using the SwissTargetPrediction platform (http://www.swisstargetprediction.ch). The SMILES representation of AVG-388 was uploaded, and the analysis was performed for the Homo sapiens target database. The results provided a ranked list of predicted protein targets based on probability values. The identified targets were categorized into functional classes, and their relevance to the study's objectives was assessed. Data visualization was completed using Python to generate a pie chart representing the distribution of target classes.

2.6. Monte Carlo Simulations and Energy Landscape Mapping

Monte Carlo simulations were conducted using NumPy (version 1.21.2) [20] to model variability in binding energies. Random samples were generated based on the mean and standard deviation of binding energies for both HIV and HCV. Additionally, a 3D energy landscape mapping was generated using Matplotlib (Matplotlib Development Team, USA) [21] to visualize the variation in binding energies across both viral targets. The binding energy differences relative to AVG-388 for each ligand were presented using bar plots, also created using Matplotlib. These visualizations provide a clear representation of ligand performance and binding energy profiles across the selected targets, aiding in the interpretation of docking and molecular interaction results.

2.7. Pharmacokinetic and Pharmacodynamic Evaluations

Pharmacokinetic and pharmacodynamic parameters of AVG-388 and FDA-approved comparator drugs were compiled through a comprehensive review of publicly available databases and peer-reviewed literature. Data for FDA-approved drugs were primarily retrieved from DrugBank (Version 5.0) software, providing detailed information on gastrointestinal (GI) absorption, plasma protein binding (PPB), volume of distribution (VD), and half-life (T1/2). Additional physicochemical properties, such as lipophilicity (LogP) and blood-brain barrier (BBB) permeability, were obtained from PubChem. Where discrepancies were observed between sources, peer-reviewed pharmacokinetic studies and FDA-approved drug labels were consulted to validate and select the most clinically relevant values. For AVG-388, an investigational compound, ADME parameters were predicted using SwissADME (http://www.swissadme.ch/) and ADMETlab 3.0 (https://admetlab3.scbdd.com/) two established *in silico* tools for evaluating pharmacokinetic properties.

3. Results and Discussion

In the presented study, the *in silico* assessment of eleven antiviral drugs and an antiviral candidate, AVG-388, against HIV and HCV revealed significant insights into their binding affinities, offering potential therapeutic implications for STDs. The relative binding energy values provided a quantitative basis for evaluating the efficacy of these antiviral agents.

From the binding affinity values presented in Table 1 (ΔG, in kcal/mol), several significant insights emerged regarding ligand performance. These values highlighted the relative strengths of interactions between the ligands and their respective targets, showcasing both the most potent binders and those with weaker affinities. Among the antivirals, sofosbuvir showed superior affinity towards the HCV target, displaying a ΔG value of -9.3 kcal/mol, underscoring its potent specificity for inhibiting HCV replication. In addition, the antiviral candidate AVG-388 demonstrated remarkably high binding affinities across all viral proteins, with ΔG values of -7.6 kcal/mol for HIV and -7.5 kcal/mol for HCV. These values indicated a strong and consistent potential for inhibiting the replication mechanisms of these viruses, positioning AVG-388 as a promising broad-spectrum antiviral candidate. In addition, ribavirin also showed notable efficacy, particularly against HCV (-8.7 kcal/mol), with the highest binding affinity.

Table 1. The relative binding energy values of ten antivirals against HIV and HCV according to *in silico* study

Ligands (Antivirals)	Binding Affinity, ΔG (kcal/mol)	
	HIV (PDB ID: 6C0J)	HCV (PDB ID: 3CJ5)
Remdesivir	- 7.3	- 6.2
Lopinavir	- 5.7	-6.3
Oseltamivir	- 6.2	- 6.2
Zanamivir	- 7.1	- 7.2
Ribavirin	- 6.3	-8.7
Nirmatrelvir	- 6.3	- 6.5
AVG – 388	-7.6	-7.5
Ritonavir	- 6.4	- 5.9
Favipiravir	-6.7	- 6.7
Molnupiravir	- 7.5	- 7.1
Entecavir	-6.1	-6.4
Sofosbuvir	-6.5	-9.3

This study also investigated the binding energies of these antiviral ligands against the target proteins of HIV and HCV employing the MM/PBSA method to calculate the binding energy values (in kJ/mol) for ligand-viral protein complexes (Table 2). For the HIV reverse transcriptase complex, the antiviral AVG-388 demonstrated a notably high binding energy of -171.15 ± 2.42 kJ/mol, indicating a strong interaction and potential inhibitory effect against the HIV reverse transcriptase. Molnupiravir and remdesivir also showed significant binding energies of -167.28 ± 3.34 kJ/mol and -162.32 ± 2.15 kJ/mol, respectively.

In the context of the HCV RdRp ns5b complex, sofosbuvir exhibited the strongest binding energy against the HCV target (-256.26 ± 2.36 kJ/mol), reinforcing its critical role in HCV therapeutic regimens. Ribavirin and AVG-388 followed with binding energies of -242.72 ± 2.24 kJ/mol and -226.21 ± 3.25 kJ/mol, respectively, highlighting their promising interactions with the HCV replication complex.

The bar plot compared the binding energies of all ligands relative to AVG-388, revealing that AVG-388 consistently outperforms other antivirals in terms of binding strength across both targets (Figure 1). The plot highlighted how AVG-388 outperforms or underperforms relative to the other ligands in terms of binding affinity, with positive values indicating weaker binding than AVG-388 and negative values reflecting stronger binding. The ligands were ordered along the x-axis, and their binding energy differences relative to AVG-388 were represented for both viral targets.

Table 2. MM/PBSA calculations of the binding energy (kJ mol^{-1}) values of ligand-protein complexes of HCV and HIV. Mean standard deviations are represented as ±

Name of Ligands (Antivirals)	MM/PBSA Binding Energy (kJ mol^{-1})	
	HIV reverse transcriptase complex	HCV RdRp NS5B protein complex
Remdesivir	-162.32 ± 2.15	-219.48 ± 3.13
Lopinavir	-118.59 ± 2.63	-182.68 ± 3.21
Oseltamivir	-127.35 ± 3.47	-176.25 ± 2.18
Zanamivir	-155.25 ± 3.42	-215.82 ± 3.38
Ribavirin	-134.21 ± 2.36	-242.72 ± 2.24
Nirmatrelvir	-132.86 ± 2.24	-191.42 ± 2.61
AVG – 388	-171.15 ± 2.42	-226.21 ± 3.25
Ritonavir	-140.56 ± 3.14	-165.13 ± 3.75
Favipiravir	-143.34 ± 2.51	-197.02 ± 2.53
Molnupiravir	-167.28 ± 3.34	-208.32 ± 2.17
Entecavir	-125.85 ± 2.16	-186.38 ± 2.84
Sofosbuvir	-141.56 ± 3.14	-256.26 ± 2.36

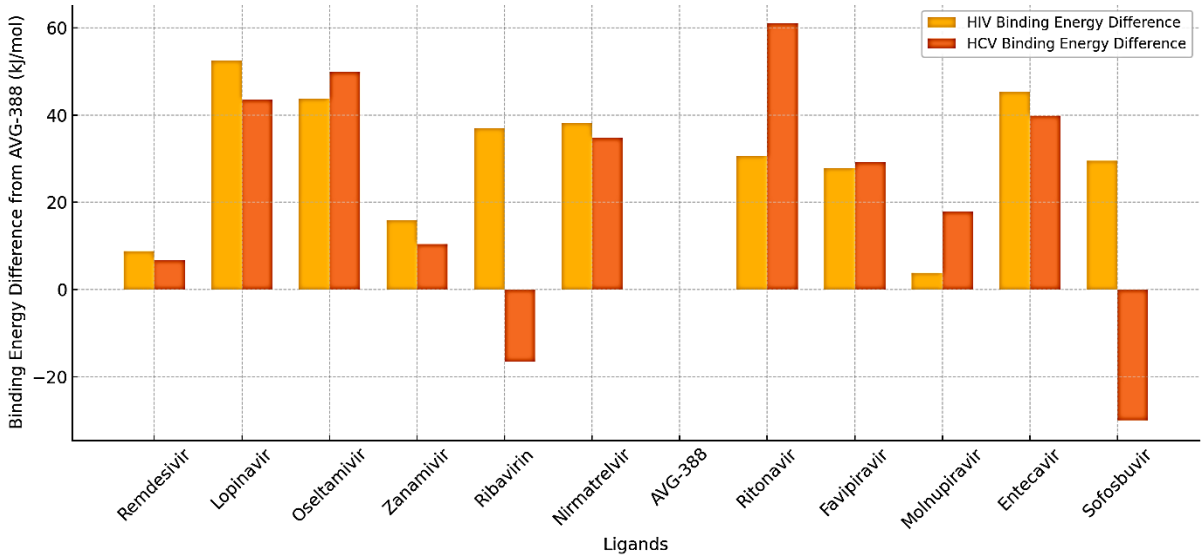

Figure 1. Binding energy differences (kJ/mol) relative to AVG-388 for antiviral ligands targeting HIV reverse transcriptase and HCV RdRp NS5B. Orange bars indicate HIV binding differences and yellow bars represent HCV binding differences. Negative values indicate stronger binding than AVG-388, while positive values reflect weaker binding

The antiviral candidate, AVG-388, served as the reference ligand in this analysis due to its consistently strong binding across both HIV and HCV. As such, most ligands exhibited positive binding energy differences, indicating that AVG-388 may bind more favorably to both viral targets. Notably, remdesivir and molnupiravir, two prominent antivirals, demonstrated moderately positive binding energy differences for both HIV and HCV. The differences suggested that they may bind less strongly to HIV and HCV proteins compared to AVG-388. On the other hand, Sofosbuvir stood out as an exception to the general trend. For HCV, Sofosbuvir indicated a negative binding energy difference, indicating that it binds more strongly to the HCV RdRp NS5B protein than AVG-388.

Lopinavir and oseltamivir exhibited substantially higher binding energy differences across both targets, suggesting that their binding affinities were significantly weaker than AVG-388. This was particularly pronounced for HCV, where their binding energy differences were notably large, highlighting their unsuitability for targeting the HCV polymerase. In addition, zanamivir and ritonavir showed the largest binding energy differences for both targets. These ligands were positioned as the weakest binders in the study, with large positive differences indicating poor binding affinity for both HIV and HCV.

Furthermore, ribavirin exhibited a relatively small

binding energy difference for HIV but a more substantial difference for HCV. This suggested that while ribavirin may exhibit moderate efficacy for HCV, its binding affinity for HIV reverse transcriptase was inferior to that of AVG-388. Similarly, nirmatrelvir showed a binding energy difference close to zero for HIV, indicating that it performed comparably to AVG-388 for this target. However, its binding energy difference for HCV was larger, indicating that its efficacy might be more limited against this target.

The bar plot demonstrated that AVG-388 consistently exhibited superior binding affinity compared to most other ligands tested, particularly across both HIV and HCV. While Sofosbuvir showed stronger binding for HCV, its weak performance against HIV confirmed its role as a highly specific HCV inhibitor rather than a broad-spectrum agent. Other ligands, such as remdesivir and molnupiravir, showed some potential for dual-target activity but remained less effective than AVG-388. Ligands with the largest positive binding energy differences, such as ritonavir and lopinavir, demonstrated limited efficacy across both targets, further supporting the potential of AVG-388 as a versatile antiviral candidate capable of inhibiting both HIV and HCV polymerases.

In the statistical analysis of ligands and HIV reverse transcriptase complex, the binding energies of ligand complexes were compared to each other, and the majority of them were found to be statistically significant ($P<0.001$). However, several comparisons emerged as non-significant (ns), indicating a potential similarity in their interaction capabilities with viral targets. Notably, the comparison between remdesivir and molnupiravir did not show a significant difference ($P=0.209$), suggesting a potential similarity in their mechanisms or efficacy against certain viral targets. Similarly, the comparison of oseltamivir vs. nirmatrelvir ($P=0.1072$) and ribavirin vs. nirmatrelvir ($P=0.9997$) also did not reveal significant differences, indicating a potential overlap in their antiviral activities. Furthermore, the comparison between AVG-388 and molnupiravir ($P=0.5634$) suggested a lack of significant disparity in their binding affinities, potentially highlighting these agents' versatility or broad-spectrum capabilities.

Similarly, the statistical analysis of binding energies of ligands in the RdRp ns5b region of HCV revealed a significant differentiation in binding energies for most comparisons, with many results showcasing P values less than 0.001, indicating a strong statistical significance. Conversely, only a few comparisons yielded ns results, specifically remdesivir vs. zanamivir ($P=0.6713$), lopinavir vs. entecavir ($P=0.6567$), nirmatrelvir vs. favipiravir ($P=0.1106$), and nirmatrelvir vs. entecavir ($P=0.2143$), indicating no significant differences in their binding affinities under the conditions tested.

In addition to demonstrating superior binding strength, an *in silico* analysis was conducted to evaluate the potential off-target effects of AVG-388. This analysis revealed that the majority of AVG-388's predicted targets fall within the "transferase" class of enzymes, accounting for 60% of the identified targets (Figure 2). Importantly, the transferase class includes key targets such as HIV reverse transcriptase and HCV RdRp NS5B, which aligned with the primary objectives of this study and confirmed the molecule's high specificity for these enzymes. Other potential off-targets included proteases (10%), kinases (8%), and a few additional biological targets with lower probabilities (6-8%). However, the binding affinity of these off-targets was significantly lower compared to the primary targets, reinforcing the high selectivity of AVG-388 for HIV and HCV enzymes. These findings validated AVG-388's promise as a potent candidate against HIV reverse transcriptase and HCV RdRp NS5B while indicating limited off-target interactions.

The multivariate regression analysis visually depicted the relationship between the binding energies of ligands for both HIV reverse transcriptase and HCV RdRp NS5B proteins and their predicted antiviral efficacy (Figure 3). The 3D plot demonstrated that binding energy acts as a critical determinant of performance, with a linear relationship between the two variables. Overall, the multivariate regression analysis solidified the role of binding energy as a primary predictor of ligand efficacy in computational antiviral studies. The plot highlighted that as binding energy decreases (becomes more negative), the predicted performance improves, confirming the inverse relationship between binding affinity and antiviral efficacy. The regression plane, shown in red, was well-fitted to the data points, each representing a ligand's binding energy values for HIV and HCV. This plane demonstrated that both HIV and HCV binding energies equally influenced the predicted efficacy, as evidenced by the slope of the plane and the uniformity of the distribution of data points. Ligands positioned closer to the regression plane like AVG-388, had high predictive accuracy based on their binding energy values.

The 3D plot of the regression model illustrated a clear linear relationship between binding energies and ligand performance, with a high R^2 value of 1.0. This value indicated a perfect fit, meaning that the binding energies of the ligands alone could fully explain their predicted efficacy in this model. This result was significant as it suggested that the binding affinities for both HIV and HCV were sufficient predictors of overall ligand performance without needing to account for additional molecular or pharmacokinetic variables. Furthermore, the spread of the data points on the x-axis (HIV binding energies) and y-axis (HCV binding energies) showed the variation in binding performance across ligands. Ligands with stronger binding affinities (lower energy values) were clustered on the lower end of the axes, corresponding to better-predicted performance. In contrast, ligands with weaker affinities were distributed towards higher energy values and exhibited lower predicted

efficacy. This analysis underscored the dual-target potential of ligands such as AVG-388, which exhibited consistently strong binding to both viral targets. It further suggested that identifying ligands with lower binding energies across multiple viral targets could be an effective strategy in broad-spectrum antiviral development.

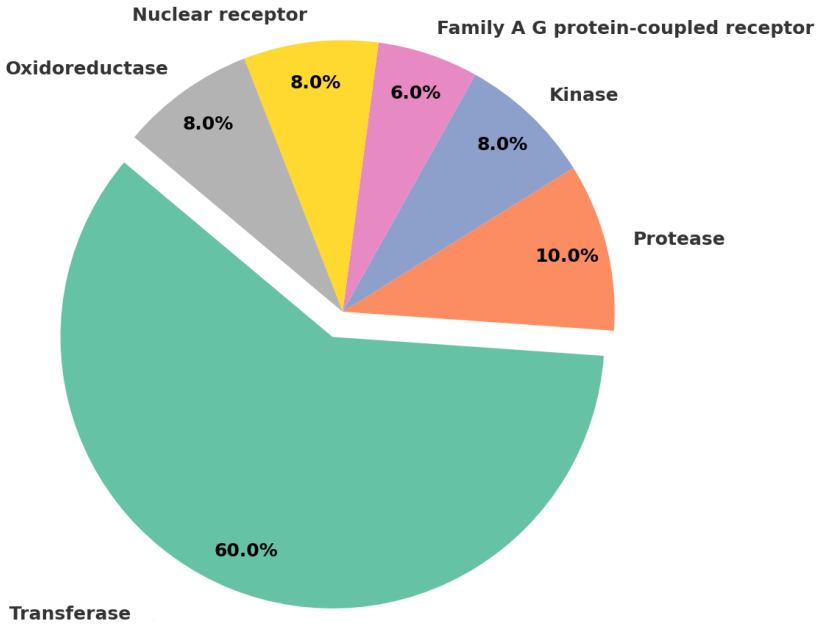

Figure 2. Pie chart illustrates the target distribution of AVG-388. The chart highlights the dominance of the transferase class among predicted targets, supporting the molecule's specificity and therapeutic potential

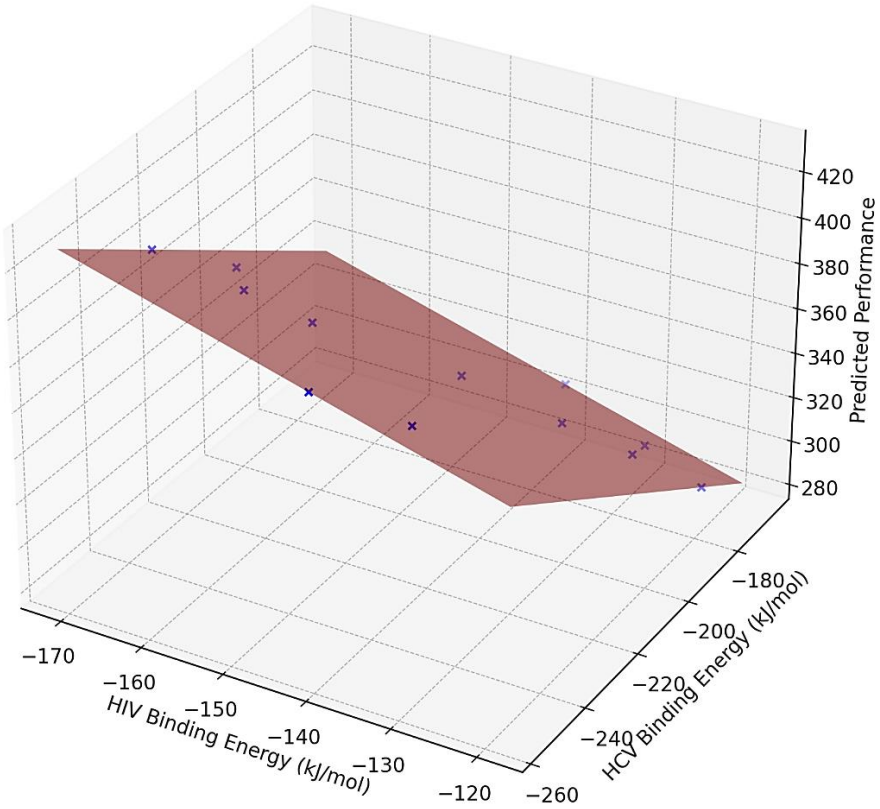

Figure 3. Multivariate regression plot showing the relationship between binding energies (kJ/mol) for HIV reverse transcriptase and HCV RdRp NS5B, and predicted ligand performance. The x-axis represents HIV binding energy, the y-axis shows HCV binding energy and the z-axis indicates predicted performance. The red plane illustrates the regression fit, highlighting that lower binding energies correlate with improved predicted performance. Ligands closer to the plane, such as AVG-388, show higher predictive accuracy based on binding energies across both targets

The 3D energy landscape mapping provided a comprehensive visualization of the binding energy variations for the twelve antiviral ligands across the HIV reverse transcriptase and HCV RdRp NS5B targets (Figure 4). The surface plot revealed that ligand binding energies differ significantly between the two viral targets, with some ligands showing broad-spectrum activity while others display target specificity. AVG-388 emerged as a strong candidate, with consistently low binding energies across both HIV and HCV targets, represented by its position on the lower plane of the energy landscape. This consistent binding affinity suggested that AVG-388 has the potential to act as a broad-spectrum antiviral, effective against both viruses. In contrast, Sofosbuvir exhibited an exceptional binding affinity for the HCV target, with a binding energy around -250 kJ/mol, but showed much weaker binding to HIV.

Furthermore, molnupiravir and remdesivir showed relatively strong binding to HIV reverse transcriptase but demonstrated weaker binding affinities for HCV, as indicated by their positioning on the landscape. Their intermediate performance across both targets suggested that while they may possess some cross-viral activity, their efficacy may be limited compared to more specific inhibitors like sofosbuvir for HCV. The landscape further revealed that ligands such as ritonavir and lopinavir, both primarily used in the treatment of HIV, had weak binding affinities for both HIV and HCV, indicating limited cross-viral potential.

The Monte Carlo simulation of binding energies provided a statistical estimation of the binding energy distributions for the twelve ligands against both HIV reverse transcriptase and HCV RdRp NS5B proteins. The density plot, which overlays histograms of the simulated binding energy values, highlighted key differences in the binding affinities between the two viral targets and underscores the potential variability in ligand performance. The x-axis represented the binding energy in kJ/mol, while the y-axis represented the density, indicating the frequency of occurrence for each binding energy value during the 1000 Monte Carlo simulation runs. The two distributions—HIV in blue and HCV in red—illustrated the variability and average binding energies for the ligands across both targets (Figure 5).

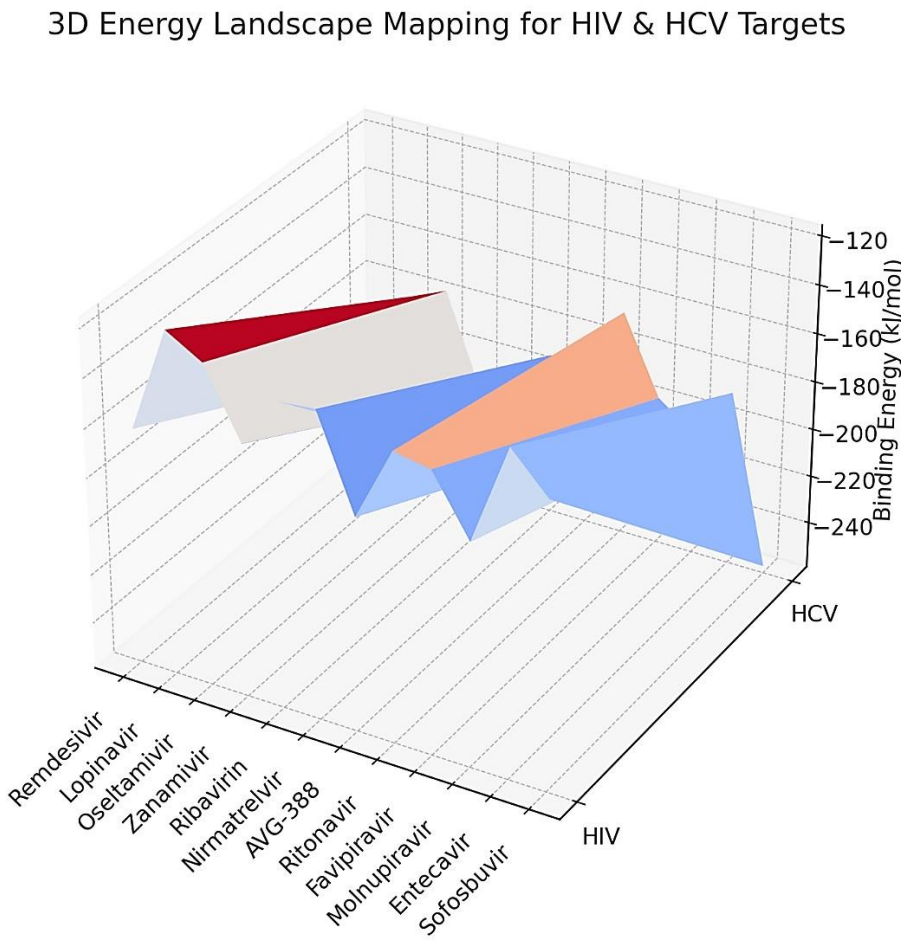

Figure 4. 3D energy landscape mapping of binding energies (kJ/mol) for HIV reverse transcriptase and HCV RdRp NS5B across different ligands. The x-axis represents the ligands, the y-axis shows the viral targets (HIV and HCV), and the z-axis reflects the binding energy. Lower regions indicate stronger binding affinity

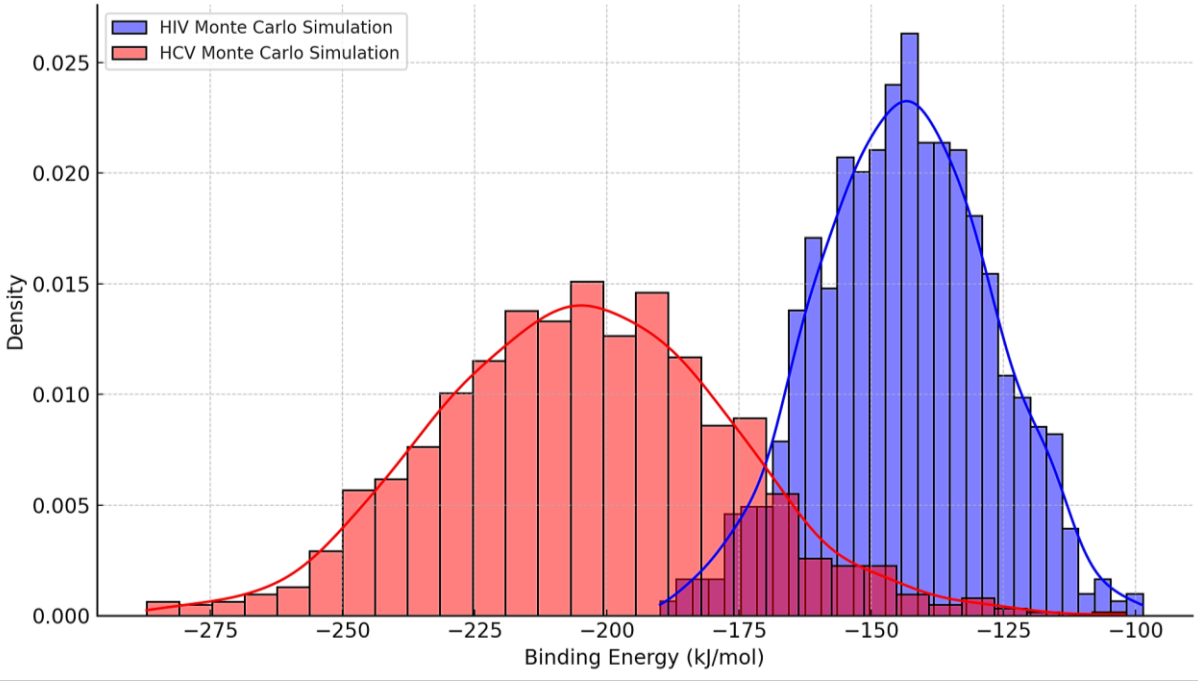

Figure 5. Monte Carlo simulation of binding energy distributions for HIV reverse transcriptase (blue) and HCV RdRp NS5B (red). The x-axis shows the binding energy (kJ/mol), while the y-axis represents the density of occurrences from the simulation

The HIV reverse transcriptase binding energy distribution (blue) displayed a normal distribution with a peak centered around -150 kJ/mol. This peak represented the most frequently observed binding energy in the simulation, with values ranging predominantly between -175 and -125 kJ/mol. The left tail of the distribution extended towards -175 kJ/mol, suggesting that a few ligands exhibited stronger binding (more negative values), with AVG-388 likely contributing to this lower range. The right tail, which extended towards -100 kJ/mol, represented weaker-binding ligands, such as lopinavir and oseltamivir, whose binding energies are much higher. The density curve for HIV binding energies was relatively sharp, indicating that there was less variability in the binding energies across the ligands. This suggested that the ligands perform more consistently for the HIV target, with most ligands clustering around similar binding energy values. The narrower range of values around the mean further suggested that there were fewer extreme outliers in terms of binding strength.

In contrast, the HCV RdRp NS5B binding energy distribution (red) was broader and slightly skewed towards the left, indicating a wider range of binding energy values for the ligands. The peak of the HCV distribution was centered around -200 kJ/mol, with values ranging from approximately -250 kJ/mol to -150 kJ/mol. The broader and flatter distribution suggested greater variability in how the ligands interact with the HCV RdRp NS5B protein. The left tail of the HCV distribution, which extended beyond -250 kJ/mol, represented the strongest binding ligands for HCV, such as Sofosbuvir, which was known for its potent inhibition of the HCV polymerase. The rightward extension of the distribution towards -150 kJ/mol represented ligands with weaker binding affinities, including those with limited efficacy against HCV.

The molecular interactions of these interactions highlighted the role of amino acid residues in the binding regions and antiviral compounds. The binding interactions of AVG-388 with the active site of HIV reverse transcriptase were examined, revealing halogen bonding facilitated by fluorine substituents with residues ARG358, GLU370, and TRP406, alongside hydrogen bonding mediated by both fluorine and carbonyl groups interacting with LYS64, LYS366, and GLN407 (Figure 6). Furthermore, electrostatic interactions contributed to the stabilization of the AVG-388 within the binding site, primarily through the aromatic rings present in AVG-388. The RdRp NS5B protein of HCV is characterized by a leucine-rich active site. Detailed examination of the binding interactions between AVG-388 and this active site highlighted the role of halogen bonding, enabled by fluorine substituents at LEU469, LEU474, and LEU536, as well as hydrogen bonding involving SER473 and ASN527 (Figure 7). Additionally, the stabilization of AVG-388 within the binding site was significantly aided by electrostatic interactions, notably through the lysine residues and the aromatic rings of AVG-388.

In addition to the interaction profile, the pharmacokinetic and pharmacodynamic profiles of AVG-388 were compared with those of FDA-approved drugs (Table 3). AVG-388 demonstrated a high GI absorption rate (92%), indicating excellent bioavailability,

comparable to Favipiravir (~94%) and higher than most other reference drugs, including Oseltamivir (~80%) and Lopinavir (~25%). Its LogP value (3.2) suggests optimal lipophilicity, providing a balance between membrane permeability and solubility while avoiding extremes seen in compounds like Ritonavir (4.8) or Zanamivir (-2.1). This positions AVG-388 as a versatile candidate for oral administration with favorable pharmacokinetics.

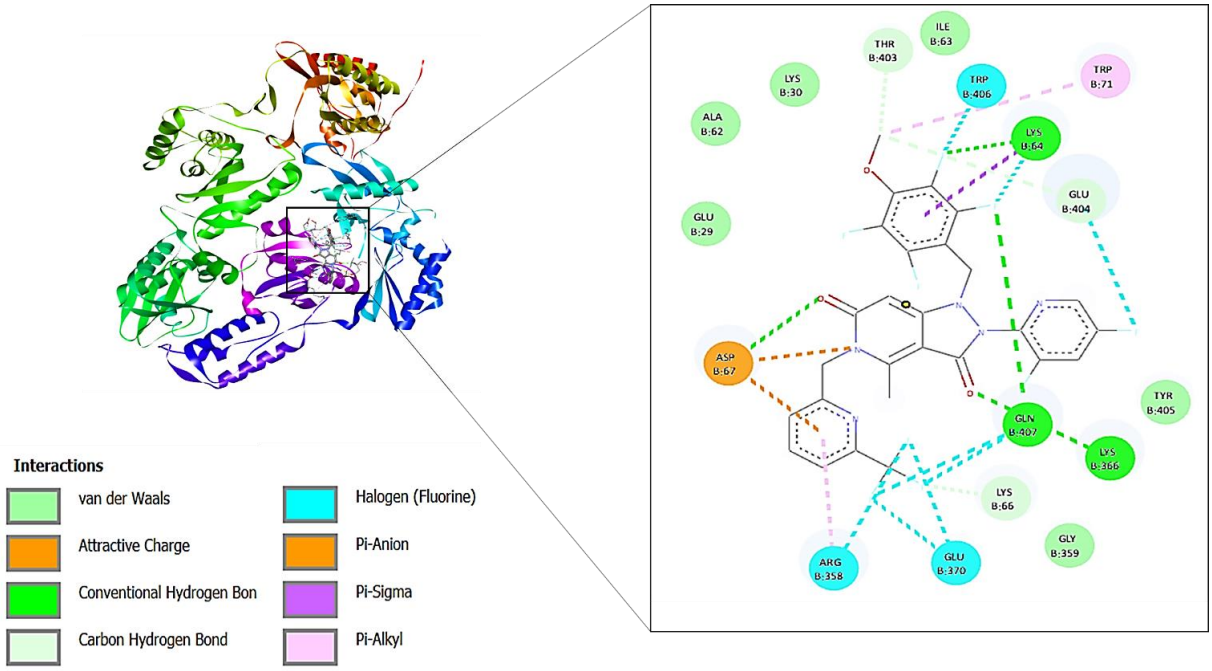

Figure 6. The binding interactions of AVG-388 in the binding region of HIV reverse transcriptase. Color-coded interactions include van der Waals forces, hydrogen bonds, and π interactions, indicating key residues involved in the ligand binding. These interactions highlight the stability and specificity of the ligand's binding within the active site

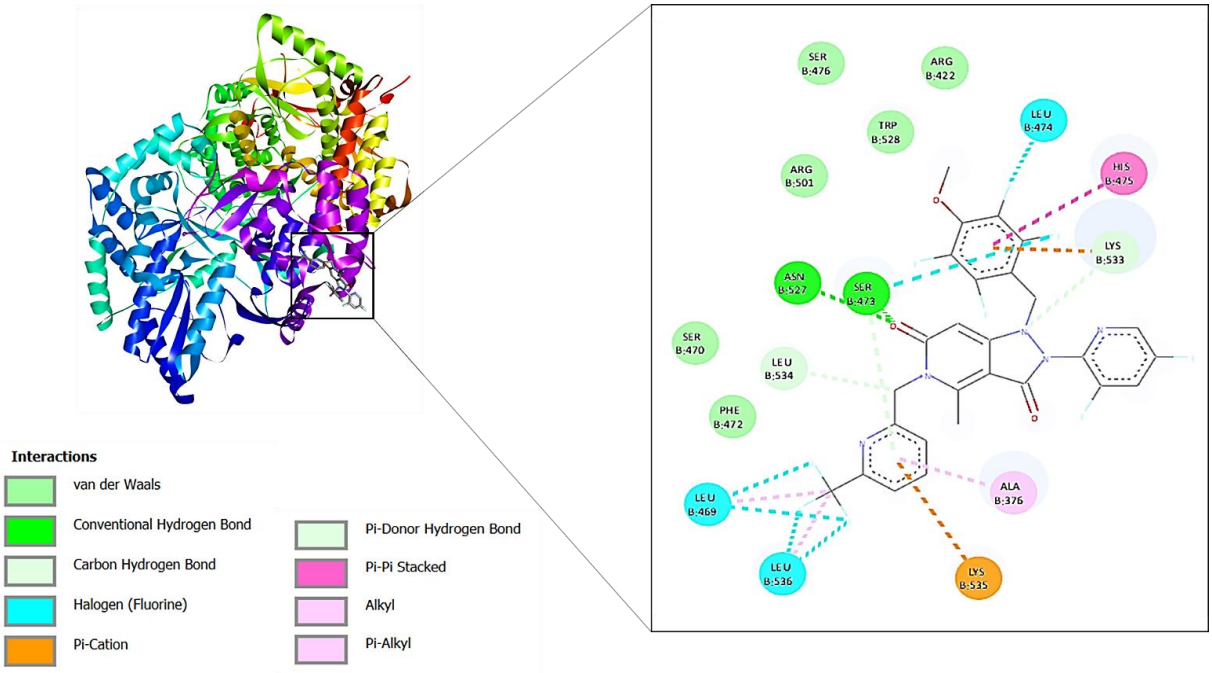

Figure 7. The binding interactions of AVG-388 with the active region of RdRp NS5B protein of HCV. The interactions include van der Waals forces, hydrogen bonds, π-alkyl interactions, and halogen bonding, which are color-coded based on the type. These interactions involve key residues within the active site, such as ARG, LEU, and ALA, highlighting the molecular stability and specificity of the ligand's binding affinity to the target protein

Table 3. Pharmacokinetic and physicochemical properties of AVG-388 and FDA-approved reference ligands

Name of Ligand	GI Absorption (%)	LogP	BBB Permeability	CYP3A4 Interaction	PPB (%)	Half-Life (hours)	VD (L/kg)
AVG-388	92	3.2	Yes	No	85	24	0.8
Remdesivir	N/A	2.1	No	Yes	88-93	~0.8	0.5
Favipiravir	~94	-0.5	No	Minimal	54	2–5	0.8–0.9
Oseltamivir	~80	1.2	No	Minimal	42	1–3	23–26
Ritonavir	~75	4.8	No	Strong Inhibitor	98–99	3–5	0.41–0.63
Lopinavir	~25	4.7	No	Metabolized by CYP3A4	98–99	5–6	0.16–0.45
Ribavirin	~64	-1.1	No	Minimal	0	9–11	2.5–5
Zanamivir	<5	-2.1	No	Minimal	10	2.5–5.1	16–41
Nirmatrelvir	~76	2.3	No	Metabolized by CYP3A4	69	6.05	104.7
Entecavir	~100 (empty stomach)	-0.6	No	Minimal	89	128–149	4.3–8.0
Sofosbuvir	~88	4.0	Yes	Minimal	88	0.4–0.5	0.81–0.97
Molnupiravir	~80	3.5	Yes	Yes	84	0.9	142

Importantly, AVG-388 displayed BBB permeability, a critical attribute for potential therapeutic applications targeting central nervous system (CNS) diseases. Among the comparators, only Sofosbuvir and Molnupiravir shared this property, whereas the majority, including Favipiravir and Remdesivir, lacked BBB permeability. This characteristic may enhance AVG-388's potential utility in treating CNS-associated conditions, expanding its therapeutic scope.

For the evaluation of their metabolism, CYP3A4 interaction analysis revealed that AVG-388 does not inhibit or undergo metabolism by CYP3A4, minimizing the risk of drug-drug interactions. In contrast, drugs such as Ritonavir and Lopinavir, which are strong CYP3A4 inhibitors, are prone to complex pharmacokinetic interactions. PPB for AVG-388 was moderate (85%), ensuring a favorable free drug concentration, unlike highly bound drugs like Ritonavir (>98%) or unbound ones like Ribavirin (0%).

AVG-388 also exhibited an ideal half-life of 24 hours, supporting once-daily dosing and ensuring sustained therapeutic activity. Comparatively, drugs such as Sofosbuvir (~0.5 hours) require more frequent administration, while Entecavir (128–149 hours) may risk prolonged accumulation. Its VD at 0.8 L/kg reflects balanced tissue penetration without excessive accumulation, contrasting with Molnupiravir's very high VD (142 L/kg), which could lead to off-target effects.

Collectively, these results highlight AVG-388's pharmacokinetic advantages, including high GI absorption, BBB permeability, minimal CYP3A4 interaction, and favorable half-life, making it a promising candidate for further development. Its ability to combine favorable pharmacokinetic properties with therapeutic flexibility underscores its potential as a novel therapeutic agent.

The emergence of resistance, driven by viral mutations that affect drug target sites, necessitates a continuous search for novel antivirals and alternative therapeutic strategies to stay ahead of evolving viral pathogens [22]. RNA viruses, including HCV and HIV, exhibit high mutation rates due to the lack of proofreading capabilities of their RdRps. These high mutation rates contribute to the rapid emergence of drug-resistant variants. Each of these viruses has specific resistance mechanisms. HIV's reverse transcriptase and integrase enzymes are prone to errors during DNA synthesis, leading to a high mutation rate [23]. Resistance to reverse transcriptase inhibitors (RTIs) can occur through mutations such as M184V that change the enzyme's active site or alter drug binding [24]. In addition, HCV resistance arises through mutations in the regions of the viral genome encoding proteins targeted by direct-acting antivirals (DAAs) [25]. The mutations in the NS5A or the NS5B protein can confer resistance to targeted inhibitors [26]. Moreover, the high genetic variability of HCV, with multiple genotypes and quasispecies within an infected individual, complicates treatment and increases the risk of resistance development [27].

Significant achievements in laboratory investigations concerning antiviral drugs and drug resistance involve the discovery of the M2 ion channel of influenza A virus (Amantadine) [28], the UL97 protein kinase of human cytomegalovirus (HCMV) (Ganciclovir) [29], and the initial elucidation of the crystal structure of HIV reverse transcriptase (Nevirapine) [30]. However, *in silico* methodologies have revolutionized the landscape of antiviral research, offering a suite of computational tools that circumvent the necessity for traditional laboratory-based assays [31]. These approaches mitigate the logistical challenges associated with physical

experimentation and significantly expedite the process of data acquisition, presenting a reliable stream of insights derived purely from computational analyses [31].

In this study, the efficacy of eleven antiviral agents and a drug candidate against two distinct STD-causing RNA viruses, namely HIV and HCV was investigated. The study presented a detailed examination of the binding affinities and energies of various antiviral agents against the target proteins of HIV and HCV utilizing molecular docking, MM/PBSA calculations, multivariate regression analysis, landscape energy mapping, and Monte Carlo simulations alongside structural representations of viral interactions. These approaches underscored the critical necessity of antiviral drugs in managing viral infections, particularly in light of the ongoing challenges posed by viral resistance mechanisms [32, 33].

The binding energy analysis of the tested ligands, as illustrated in the bar plot and subsequent statistical comparisons, highlighted AVG-388's superior binding affinity across both HIV and HCV targets. AVG-388 consistently outperformed other antiviral drugs in terms of binding strength. This suggested that AVG-388 has the potential to serve as an effective broad-spectrum antiviral, capable of inhibiting both HIV reverse transcriptase and HCV RdRp NS5B polymerase. In addition, remdesivir and molnupiravir, both FDA-approved antivirals known for their efficacy in clinical settings [34-36], displayed moderate positive binding energy differences relative to AVG-388. While these compounds were recognized for their antiviral properties, their weaker binding affinities compared to AVG-388 suggested that they may not possess the same dual-target inhibition potential as the candidate molecule.

Sofosbuvir, however, presented an exception in the analysis. For the HCV target, Sofosbuvir demonstrated a negative binding energy difference, indicating a stronger binding affinity for the HCV RdRp NS5B protein compared to AVG-388. This result was consistent with Sofosbuvir’s well-documented clinical efficacy as a potent HCV inhibitor [37]. However, its large positive binding energy difference for HIV suggested that Sofosbuvir may be significantly less effective against HIV reverse transcriptase, underscoring its specificity for HCV. The data reinforced the understanding that Sofosbuvir, while highly effective for HCV, may lack the versatility needed for dual-target antiviral applications. Moreover, Ribavirin, a broad-spectrum antiviral [38], demonstrated a relatively small binding energy difference for HIV but a larger difference for HCV, suggesting that while it may exhibit moderate efficacy against HCV, it does not perform as well as AVG-388 for HIV. Similarly, Nirmatrelvir, which showed a binding energy difference close to zero for HIV, performed comparably to AVG-388 for this target, though its weaker performance for HCV indicates its limited cross-viral potential.

The statistical data of binding energies of some STD-related RNA virus complexes indicated substantial variations in the effectiveness of different antivirals, with certain drugs like entecavir and sofosbuvir demonstrating noteworthy binding affinities and energies against specific viral targets. This variability not only highlighted the potential for tailored antiviral therapy based on the viral genotype but also emphasized the importance of alternative candidates.

The multivariate regression analysis provided further clarity on the role of binding energy as a predictor of antiviral efficacy. The regression plot illustrated a near-perfect linear relationship between binding energies for both HIV and HCV, with a strong correlation between more negative binding energies and improved predicted performance. This finding suggested that binding energies alone are reliable predictors of ligand efficacy, eliminating the need to consider additional molecular variables. The data points clustered closer to the regression plane, such as those representing AVG-388, confirmed the ligand's dual-target potential, further supporting its candidacy as a broad-spectrum antiviral. In contrast, ligands with weaker binding affinities, such as ritonavir and oseltamivir, were positioned farther from the plane, indicating limited efficacy.

The 2D and 3D energy landscape mapping methods are frequently used in previous research, offering a detailed view of the energy states a ligand can adopt during its interaction with a protein. Moreover, 3D energy landscapes can reveal if a drug is likely to bind well to multiple targets, such as in dual-target antivirals, by showing areas of the landscape where different viral proteins share similar binding characteristics [39, 40]. Similarly, in the present study, the 3D energy landscape mapping highlighted AVG-388’s strong performance across both HIV and HCV targets. In contrast, Sofosbuvir exhibited an exceptional binding affinity for HCV but weak binding to HIV, confirming its role as a specific HCV inhibitor. The intermediate performance of Remdesivir and Molnupiravir across both targets further suggested that while these drugs may have some cross-viral activity, they remain less effective than AVG-388, particularly in terms of dual-target binding.

As indicated in previous research, Monte Carlo simulations can help predict how consistently a ligand will bind to a target protein. By modeling multiple interaction scenarios, the simulation helps estimate the probability of achieving a stable and strong binding, which is critical for drug efficacy [41]. In this study, as shown in the Monte Carlo simulation model, the HIV distribution was narrower and centered at a higher binding energy value (-150 kJ/mol), suggesting that ligands generally exhibited weaker binding to HIV compared to HCV. In contrast, the HCV distribution was broader and centered at a lower energy value (-200 kJ/mol), indicating that ligands tend to bind more strongly to HCV, but with greater variability in their performance. This variability in

the HCV binding energies suggested that while some ligands, such as sofosbuvir, were highly effective at targeting HCV, others may perform less consistently.

The overlap between the two distributions around -175 kJ/mol represents ligands that have comparable binding affinities for both HIV and HCV, potentially indicating dual-target activity. Ligands such as AVG-388, which perform well for both targets, likely fall within this region of overlap, reinforcing their potential as broad-spectrum antivirals.

The translational potential of these computational findings is crucial to progress from computational predictions to clinical applications, necessitating a clear pathway for further validation and development. The computationally predicted pharmacokinetic and binding properties of AVG-388 must first be validated through *in vitro* studies, such as enzyme inhibition assays, to confirm its activity against the target enzymes. Following this, *in vivo* pharmacokinetic studies in appropriate animal models are required to verify absorption, distribution, metabolism, and excretion (ADME) profiles while assessing preliminary safety and efficacy. Structural optimization and formulation development may be necessary to enhance bioavailability and target specificity, ensuring stable delivery for oral or parenteral administration. Comprehensive toxicology studies, including dose-escalation and long-term safety assessments, will identify potential adverse effects and establish the therapeutic index. These steps provide a clear roadmap to bridge computational predictions and real-world clinical applications, underscoring the therapeutic potential of AVG-388.

4. Conclusions

The comprehensive investigation into the binding affinities and energies of AVG-388, alongside other FDA-approved antiviral agents against the target proteins of HIV and HCV, elucidated the significant potential and versatility of AVG-388 in the context of antiviral therapy for STDs. In addition, its potential for synergistic use with existing therapies could significantly impact the management and treatment of viral infections, particularly in the face of evolving resistance mechanisms. This study has some limitations indicating the necessity for subsequent *in vitro* investigations to provide more comprehensive data. The findings provide initial insights conducive to future clinical trials, suggesting the potential suitability of employing AVG-388 in addressing STDs.

Conflict of Interest Statement

The authors declare no conflict of interest.

REFERENCES

[1] Wagenlehner F. M., Brockmeyer N. H., Discher T., Friese K., Wichelhaus T. A., "The Presentation, Diagnosis, and Treatment of Sexually Transmitted Infections," *DtschArztebl Int.*, vol. 113, no. 1-02, pp. 11–22, 2016.

[2] UNAIDS, "Global HIV & AIDS Statistics — Fact Sheet," Available from: https://www.unaids.org/en/resources/fact-sheet, 2023.

[3] World Health Organization, "HIV/AIDS Data and Statistics," Available from: https://www.who.int/news-room/fact-sheets/detail/hiv-aids, 2023.

[4] Rowley J., Vander Hoorn S., Korenromp E., Low N., Unemo M., Abu-Raddad L. J., Chico R. M., Smolak A., Newman L., Gottlieb S., Thwin S. S., Broutet N., Taylor M. M., "Chlamydia, Gonorrhoea, Trichomoniasis, and Syphilis: Global Prevalence and Incidence Estimates, 2016," *Bulletin of the World Health Organization*, vol. 97, no. 8, pp. 548–562P, 2019. DOI: 10.2471/BLT.18.228486.

[5] World Health Organization, "Hepatitis C Fact Sheet," Available from: https://www.who.int/news-room/fact-sheets/detail/hepatitis-c, 2023.

[6] Elena S. F., Sanjuán R., "Adaptive Value of High Mutation Rates of RNA Viruses: Separating Causes from Consequences," *Journal of Virology*, vol. 79, no. 18, pp. 11555–11558, 2005. DOI: 10.1128/JVI.79.18.11555-11558.2005.

[7] Sanjuán R., Domingo-Calap P., "Mechanisms of Viral Mutation," *Cellular and Molecular Life Sciences*, vol. 73, no. 23, pp. 4433–4448, 2016. DOI: 10.1007/s00018-016-2299-6.

[8] Perrin L., Telenti A., "HIV Treatment Failure: Testing for HIV Resistance in Clinical Practice," *Science*, vol. 280, no. 5371, pp. 1871–1873, 1998. DOI: 10.1126/science.280.5371.1871.

[9] Tabata K., Neufeldt C. J., Bartenschlager R., "Hepatitis C Virus Replication," *Cold Spring Harbor Perspectives in Medicine*, vol. 10, no. 3, a037093, 2020. DOI: 10.1101/cshperspect.a037093.

[10] Workowski K. A., Bachmann L. H., Chan P. A., Johnston C. M., Muzny C. A., Park I., Reno H., Zenilman J. M., Bolan G. A., "Sexually Transmitted Infections Treatment Guidelines, 2021," *MMWR. Recommendations and Reports*, vol. 70, no. 4, pp. 1–187, 2021. DOI: 10.15585/mmwr.rr7004a1.

[11] Islam T., Hasan M., Rahman M. S., Islam M. R., "Comparative Evaluation of Authorized Drugs for Treating Covid-19 Patients," *Health Science Reports*, vol. 5, no. 4, e671, 2022. DOI: 10.1002/hsr2.671.

[12] Reis S., Metzendorf M. I., Kuehn R., Popp M., Gagyor I., Kranke P., Meybohm P., Skoetz N., Weibel S., "Nirmatrelvir Combined with Ritonavir for Preventing and Treating COVID-19," *Cochrane Database of Systematic Reviews*, vol. 11, no. 11, CD015395, 2023. DOI: 10.1002/14651858.CD015395.pub3.

[13] De Clercq E., Li G., "Approved Antiviral Drugs Over the Past 50 Years," *Clinical Microbiology Reviews*, vol. 29, no. 3, pp. 695–747, 2016. DOI: 10.1128/CMR.00102-15.

[14] Ison M. G., "Antiviral Treatments," *Clinics in Chest Medicine*, vol. 38, no. 1, pp. 139–153, 2017. DOI: 10.1016/j.ccm.2016.11.008.

[15] Sourimant J., Lieber C. M., Yoon J. J., Toots M., Govindarajan M., Udumula V., Sakamoto K., Natchus M. G., Patti J., Vernachio J., Plemper R. K., "Orally Efficacious Lead of the AVG Inhibitor Series Targeting a Dynamic Interface in the Respiratory Syncytial Virus Polymerase," *Science Advances*, vol. 8, no. 25, eabo2236, 2022. DOI: 10.1126/sciadv.abo2236.

[16] Maiocchi A., "Genetic Algorithms in Molecular Modeling: A Review," *Data Handling in Science and Technology*, vol. 23, pp. 109–139, 2003.

[17] Simmonett A. C., Brooks B. R., "A Compression Strategy for Particle Mesh Ewald Theory," *The Journal of Chemical Physics*, vol. 154, no. 5, 054112, 2021. DOI: 10.1063/5.0040966.

[18] Sultanoglu N., Erdag E., Ozverel C. S., "A Single Antiviral for a Triple Epidemic: Is It Possible?," *Future Virology*, vol. 18, no. 10, pp. 633-642, 2023.

[19] Ashiabi G. S., "From Scratch: A Didactic Example of Multivariate Regression in Python," *The Quantitative Methods for Psychology*, vol. 20, no. 2, pp. 186–204, 2024. DOI: 10.20982/tqmp.20.2.p186.

[20] Holman J. O., Hacherl A., "Teaching Monte Carlo Simulation with Python," *Journal of Statistics and Data Science Education*, vol. 31, no. 1, pp. 33–44, 2023. DOI: 10.1080/26939169.2022.2111008.

[21] Wilkinson C. J., Mauro J. C., "Explorer.py: Mapping the Energy Landscapes of Complex Materials," *SoftwareX*, vol. 14, 100683, 2021.

[22] Tanner E. J., Liu H. M., Oberste M. S., Pallansch M. S., Collett M. S., Kirkegaard K., "Dominant Drug Targets Suppress the Emergence of Antiviral Resistance," *Elife*, vol. 3, e03830, 2014. DOI: 10.7554/eLife.03830.

[23] Chen S., Wu J., Yang X., Sun Q., Liu S., Rashid F., Dzakah E. E., Wang H., Wang J., Gong P., Tang S., "RNA-Dependent RNA Polymerase of the Second Human Pegivirus Exhibits a High-Fidelity Feature," *Microbiology Spectrum*, vol. 10, no. 5, e0272922, 2022. DOI: 10.1128/spectrum.02729-22.

[24] Xu H. T., Martinez-Cajas J. L., Ntemgwa M. L., Coutsinos D., Frankel F. A., Brenner B. G., Wainberg M. A., "Effects of the K65R and K65R/M184V Reverse Transcriptase Mutations in Subtype C HIV on Enzyme Function and Drug Resistance," *Retrovirology*, vol. 6, pp. 1–14, 2009. DOI: 10.1186/1742-4690-6-14.

[25] Aldunate F., Echeverría N., Chiodi D., López P., Sánchez-Cicerón A., Fajardo A., Soñora M., Cristina J., Hernández N., Moreno P., "Pretreatment Hepatitis C Virus NS5A/NS5B Resistance-Associated Substitutions in Genotype 1 Uruguayan Infected Patients," *Disease Markers*, vol. 2018, Article ID 2514901, 2018. DOI: 10.1155/2018/2514901.

[26] Andrade E., Rocha D., Fontana-Maurell M., Costa E., Ribeiro M., Godoy D. T., Ferreira A. G. P., Tanuri A., Brindeiro R., Alvarez P., "Resistance Mutations of NS3 and NS5b in Treatment-Naïve Patients Infected with Hepatitis C Virus in Santa Catarina and Rio Grande do Sul States, Brazil," *Genetics and Molecular Biology*, vol. 43, no. 1, e20180237, 2020. DOI: 10.1590/1678-4685-GMB-2018-0237.

[27] Argentini C., Genovese D., Dettori S., Rapicetta M., "HCV Genetic Variability: From Quasispecies Evolution to Genotype Classification," *Future Microbiology*, vol. 4, no. 3, pp. 359-373, 2009. DOI: 10.2217/fmb.09.8.

[28] Musharrafieh R., Ma C., Wang J., "Discovery of M2 Channel Blockers Targeting the Drug-Resistant Double Mutants M2-S31N/L26I and M2-S31N/V27A from the Influenza A Viruses," *European Journal of Pharmaceutical Sciences*, vol. 141, 105124, 2020. DOI: 10.1016/j.ejps.2019.105124.

[29] Steingruber M., Marschall M., "The Cytomegalovirus Protein Kinase pUL97: Host Interactions, Regulatory Mechanisms and Antiviral Drug Targeting," *Microorganisms*, vol. 8, no. 4, 515, 2020. DOI: 10.3390/microorganisms8040515.

[30] Das K., Martinez S. E., Bauman J. D., Arnold E., "HIV-1 Reverse Transcriptase Complex with DNA and Nevirapine Reveals Non-Nucleoside Inhibition Mechanism," *Nature Structural & Molecular Biology*, vol. 19, no. 2, pp. 253–259, 2012. DOI: 10.1038/nsmb.2223.

[31] Moradi M., Golmohammadi R., Najafi A., Moosazadeh Moghaddam M., Fasihi-Ramandi M., Mirnejad R., "A Contemporary Review on the Important Role of In Silico Approaches for Managing Different Aspects of COVID-19 Crisis," *Informatics in Medicine Unlocked*, vol. 28, 100862, 2022. DOI: 10.1016/j.imu.2022.100862.

[32] Du S., Hu X., Menéndez-Arias L., Zhan P., Liu X., "Target-Based Drug Design Strategies to Overcome Resistance to Antiviral Agents: Opportunities and Challenges," *Drug Resistance Updates*, vol. 73, 101053, 2024. DOI: 10.1016/j.drup.2024.101053.

[33] Domingo E., García-Crespo C., Soria M. E., Perales C., "Viral Fitness, Population Complexity, Host Interactions, and Resistance to Antiviral Agents," *Current Topics in Microbiology and Immunology*, vol. 439, pp. 197–235, 2023. DOI: 10.1007/978-3-031-15640-3_6.

[34] Del Borgo C., Garattini S., Bortignon C., Carraro A., Di Trento D., Gasperin A., Grimaldi A., De Maria S. G., Corazza S., Tieghi T., Belvisi V., Kertusha B., De Masi M., D'Onofrio O., Bagaglini G., Bonanni G., Zuccalà P., Fabietti P., Tortellini E., Guardiani M., … Latina Covid-Group, "Effectiveness, Tolerability and Prescribing Choice of Antiviral Molecules Molnupiravir, Remdesivir and Nirmatrelvir/r: A Real-World Comparison in the First Ten Months of Use," *Viruses*, vol. 15, no. 4, 1025, 2023. DOI: 10.3390/v15041025.

[35] Santoro M. G., Carafoli E., "Remdesivir: From Ebola to COVID-19," *Biochemical and Biophysical Research Communications*, vol. 538, pp. 145–150, 2021. DOI: 10.1016/j.bbrc.2020.11.043.

[36] Tian L., Pang Z., Li M., Lou F., An X., Zhu S., Song L., Tong Y., Fan H., Fan J., "Molnupiravir and Its Antiviral Activity Against COVID-19," *Frontiers in Immunology*, vol. 13, 855496, 2022. DOI: 10.3389/fimmu.2022.855496.

[37] Bhatia H. K., Singh H., Grewal N., Natt N. K., "Sofosbuvir: A Novel Treatment Option for Chronic Hepatitis C Infection," *Journal of Pharmacology &*

Pharmacotherapeutics, vol. 5, no. 4, pp. 278–284, 2014. DOI: 10.4103/0976-500X.142464.

[38] Snell N. J., "Ribavirin--Current Status of a Broad Spectrum Antiviral Agent," *Expert Opinion on Pharmacotherapy*, vol. 2, no. 8, pp. 1317–1324, 2001. DOI: 10.1517/14656566.2.8.1317.

[39] Baidya A. T., Kumar A., Kumar R., Darreh-Shori T., "Allosteric Binding Sites of Aβ Peptides on the Acetylcholine Synthesizing Enzyme ChAT as Deduced by In Silico Molecular Modeling," *International Journal of Molecular Sciences*, vol. 23, no. 11, 6073, 2022. DOI: 10.3390/ijms23116073.

[40] Liu Q., Herrmann A., Huang Q., "Surface Binding Energy Landscapes Affect Phosphodiesterase Isoform-Specific Inhibitor Selectivity," *Computational and Structural Biotechnology Journal*, vol. 17, pp. 101–109, 2018. DOI: 10.1016/j.csbj.2018.11.009.

[41] Cole D. J., Tirado-Rives J., Jorgensen W. L., "Molecular Dynamics and Monte Carlo Simulations for Protein-Ligand Binding and Inhibitor Design," *Biochimica et Biophysica Acta*, vol. 1850, no. 5, pp. 966–971, 2015. DOI: 10.1016/j.bbagen.2014.08.018.